

## Efficient 2D Model of Flow Distribution in Dense Tube Bundles

Vojtěch Turek\*, Dominika Fialová, Zdeněk Jegla, Bohuslav Kilkovský

Institute of Process and Environmental Engineering, Faculty of Mechanical Engineering, Brno University of Technology, Technická 2, 616 69 Brno, Czech Republic.  
 turek@fme.vutbr.cz

It is imperative that flow distribution is considered while designing heat exchanger tube bundles because it greatly influences equipment performance. What is more, a wide range of operating issues can occur if the distribution is significantly non-uniform. Since pressure gradients which, in fact, govern flow distribution can be adjusted via shape optimisation of individual parts of the flow system, such an action can not only improve performance but also increase reliability of the apparatus. Still, an efficient and accurate-enough flow model has to be available in order for the resulting optimisation model to be viable in terms of engineering practice.

Heat exchangers often feature dense tube bundles which cannot be properly described via available simplified 1D models. Utilisation of computational fluid dynamics (CFD) or other computationally-intensive approaches, on the other hand, is not feasible either due to unacceptably long optimisation times. An efficient 2D flow distribution and pressure drop model is therefore presented. Additionally, a comparison of data obtained with the model for several tube bundle geometries and the corresponding data yielded by CFD is provided.

### 1. Introduction

Nowadays – in the era of relatively cheap computing power – flow distribution is usually predicted numerically via computational fluid dynamics (CFD). Although this approach yields high-quality data, the times required to get those data are still quite long. Considering heat transfer equipment, one can easily find CFD studies concerned with air coolers (Osley et al., 2014), shell-and-tube heat exchangers (Mohammadi and Malayeri, 2013), heat recovery steam generators (Galindo-García et al., 2014), plate-fin exchangers (Zhang et al., 2015), or flat-tube cryogenic heat exchangers (Kim and Byun, 2013) to name just a few. Given the fact that the main purpose of these evaluations often is to obtain data for shape optimisation of the equipment, it is obvious that the resulting optimisation processes are not only time-consuming but also far from effortless.

Another possible – and sometimes taken – route is to work with a one-dimensional representation of the actual geometry and utilise a largely simplified flow model containing artificial pressure regain coefficients (Pustylnik et al., 2010). These coefficients are necessary because momentum changes due to splitting or combining of flows at the branching points are not considered by the original coefficient-free algebraic flow equations. In this manner one gets a model whose implementation in an automatic shape optimisation algorithm is easy and straightforward. Although this kind of approach can lead to promising results as shown for example by Turek et al. (2011), in their essence these models still work with one-dimensional (or quasi-1D) representations of the respective flow systems and hence their accuracy would most probably suffer when presented with a more complex geometry.

Lastly, one could employ a more refined model utilising partial differential equations evaluated on a simplified spatially discretised representation of the original apparatus. As shown by Turek et al. (2014), such an approach results in very efficient and reasonably accurate quasi-1D models which can take into account incremental changes in temperature (e.g. due to non-uniform heat flux) as well as in other quantities. That is why the present paper picks up where Turek et al. (2014) left off and aims to generalise the quite accurate model discussed therein from the quasi-1D mesh approach to the quasi-3D mesh approach which should, in turn, ensure reasonably fast flow evaluation while providing added accuracy for systems with geometries being further from quasi-1D ones.

## 2. Mathematical model

In principle, the equations utilised in the present model are identical to those used by Turek et al. (2014). Here, however, structure of the model must make provisions for the higher dimension of the spatially discretised geometry and the facts that now (i) each of the equations must be written for two interconnected nodes in a 2D (or quasi-3D) mesh instead of two neighbouring points in a 1D (or quasi-1D) channel segment and (ii) each mesh node connects up to four mesh edges.

Since there is no point in repeating all the derivation steps and the supplementary equations, please refer to Turek et al. (2014) for a detailed description of the process. As an example of how some of the resulting equations look like, however, let us imagine two nodes, “1” and “2”, interconnected by a mesh edge. Let also “1” be the originating node and “2” the terminating node. Then, after all the necessary equation rearrangements and simplifications we would get

$$\frac{\partial p}{\partial l} = \left[ \frac{\lambda}{2D_h} \left( 1 + \frac{\kappa - 1}{\kappa} \frac{\rho_1 v_1^2}{p_1} \right) - \frac{g \cos \varphi}{v_1^2} - \frac{1}{A_1} \frac{\partial A}{\partial l} - \frac{\delta}{\rho_1 v_1 A_1} \right] \left( \frac{1}{\kappa p_1} - \frac{1}{\rho_1 v_1^2} \right)^{-1} \quad (1)$$

for a pressure gradient between the two nodes. In the equation above, subscript “1” indicates value of a quantity at the node “1”,  $p$  denotes pressure,  $l$  length of the interconnecting edge,  $\lambda$  Darcy friction factor,  $D_h$  hydraulic diameter of the virtual flow channel,  $\kappa$  heat capacity ratio,  $\rho$  density,  $g$  standard gravity,  $\varphi$  the angle of inclination of the edge from the direction of  $g$ ,  $v$  mean flow velocity,  $A$  cross-sectional area of the virtual flow channel, and  $\delta$  the amount of fluid that leaves our control volume between the originating and the terminating node ( $\delta$  is positive if fluid leaves the control volume, otherwise it is negative). Similarly, from the first law of thermodynamics and because in this simplified case we assume that heat is generated only due to internal friction in the fluid, we would obtain

$$\frac{\partial q}{\partial l} = c_v \frac{\partial T}{\partial l} - \frac{p_1}{\rho_1^2} \frac{\partial \rho}{\partial l} \quad (2)$$

for a temperature gradient between nodes “1” and “2”. Here,  $\partial q$  denotes generated heat,  $c_v$  specific heat capacity at constant volume, and  $T$  thermodynamic temperature. Obviously, all the derived partial differential equations need to be converted to their difference representations but that is in its essence a trivial matter and information on this can be found in numeric-oriented literature.

### 2.1 Applicable tube bundle geometry types

The model has been developed without regard to any specific tube bundle arrangement and as such it should generally be able to handle arbitrary placement of tubes in a bundle. In other words, all the three common arrangements (inline – 90°, staggered – 60° and 45°) can be evaluated quite effortlessly by simply providing a few pieces of information: the type of arrangement (inline or staggered), longitudinal and transversal tube pitches, number of tube rows, and numbers of tubes per each of the rows (which is necessary because staggered rows are sometimes made one tube shorter).

The only limitation of the model is that the tubes must not be placed too sparsely, that is, longitudinal and transversal tube pitches must not be too large. This is due to the fact that the model assumes the tube sheet to be a porous layer. Even though we have not yet investigated the behaviour of the model in case of sparse bundles, it is reasonable to assume that the accuracy would decrease rather significantly.

## 3. Software implementation of the model

The model has been implemented in a command-line flow simulation tool developed in Java (Oracle, 2015) and as such no graphical user interface is available yet. A simple quasi-3D mesh is produced automatically according to the provided input data (tube pitches etc.), that is, the tube sheet is discretised in 2D (see Figure 1) while the tubes – connected to the tube sheet 2D mesh – are represented via 1D meshes. Because meshes produced this way are quite small, sequential approach to flow evaluation has been selected. In other words, the equations are evaluated sequentially on a per-node basis until convergence is reached. Physical properties of the fluid (density, dynamic viscosity, etc.) are always calculated ad hoc with respect to actual temperature and pressure to increase accuracy of the model.

Because the model is rather uncomplicated in its nature, implementing it in a geometry optimisation algorithm should be relatively straightforward. The given optimisation domain could then be searched using various algorithms depending on its actual dimension – see for example the methods mentioned in (Turek et al., 2014).

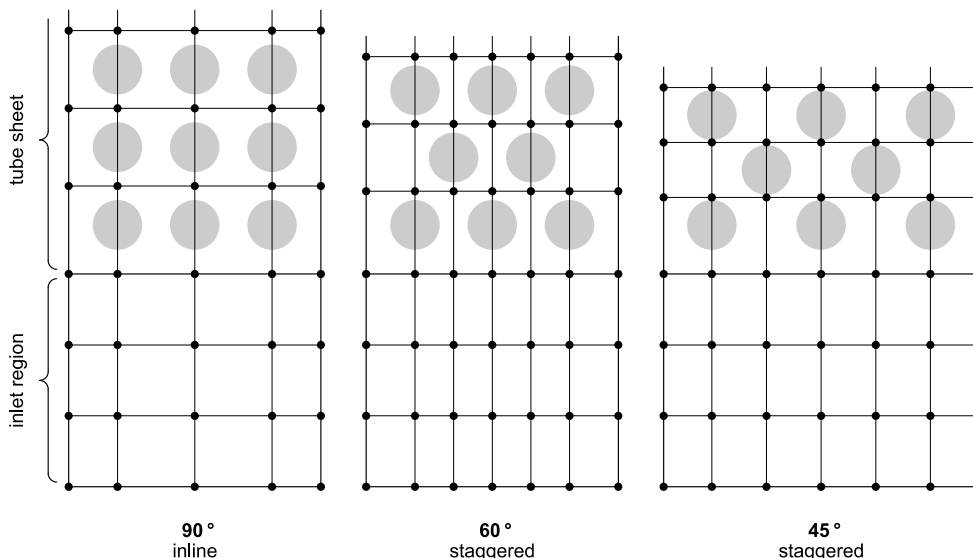


Figure 1: Automatically generated 2D tube sheet and inlet region meshes corresponding to the three common tube bundle arrangements with three (90 °) or five (60 ° and 45 °) tube rows

### 3.1 Comparison of sample results and data obtained with ANSYS Fluent

The simulation tool discussed in the previous section was used to predict flow behaviour in several testing geometries for which also data from ANSYS Fluent (ANSYS Inc., 2013) had been available. The following setup of ANSYS Fluent cases was used:

- pressure-based solver with absolute velocity formulation, second-order implicit transient formulation (if applicable), and double-precision;
- realizable  $k-\epsilon$  model with standard wall functions and energy equation;
- SIMPLE pressure-velocity coupling;
- Green-Gauss node based gradient calculation;
- spatial discretisation: second order for pressure, second order upwind for density, momentum, turbulent kinetic energy, turbulent dissipation rate, and energy.

Two test flow distribution systems will be featured in this paper. The first one was rather simple with a tube bundle consisting of two rows of 20 tubes each. Inline (90 °) arrangement was used in this case (see Figure 2). The second flow system contained five staggered tube rows of 10 tubes each with the 60 ° arrangement (see Figure 3). The respective geometry data can be found in Table 1 while flow data are listed in Table 2. Figures 4 and 5 then show comparisons of tube mass flow rates yielded by the simulation tool and the corresponding data from ANSYS Fluent obtained with both steady and fully converged unsteady computations. As for mesh fineness, in all Fluent cases mesh was fine-tuned in order to reach favourable values of  $y^+$  and thus make sure that the results were not distorted.

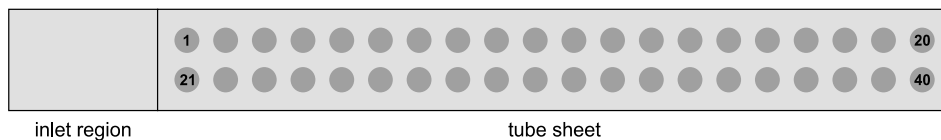


Figure 2: Top view of the first test flow system; numbers indicate tube IDs

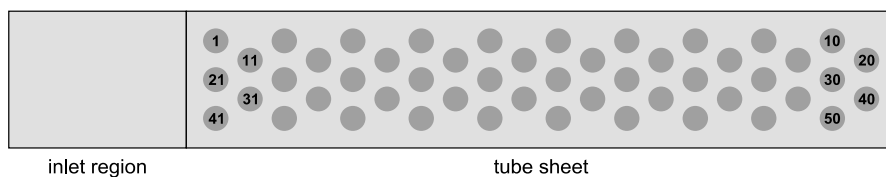


Figure 3: Top view of the second test flow system; numbers indicate tube IDs

Table 1: Geometry data related to the test systems

	Flow system I	Flow system II
Tube sheet: width, m	0.040	0.055
length, m	0.320	0.280
Inlet region length, m	0.060	0.070
Header height, m	0.040	0.055
Tube bundle: arrangement	inline / 90°	staggered / 60°
number of tube rows	2	5
number of tubes in a row	20	10
Tubes: inner diameter, m	0.010	0.010
length, m	1.000	1.000
outlet region length, m	0.100	0.100

Table 2: Flow data related to the test systems

	Flow system I			Flow system II		
	Simulation tool	Fluent (steady)	Fluent (unsteady)	Simulation tool	Fluent (steady)	Fluent (unsteady)
Fluid*	air			air		
Mass flow rate*, kg/s	0.10			0.25		
Pressure: inlet, Pa	102,453.9*	102,415.7	102,453.9	106,798.9*	109,011.0	106,798.9
outlet, Pa	100,534.1	101,325.0*	101,325.0*	99,055.0	101,325.0*	101,325.0*
drop, Pa	1,919.8	1,090.7	1,128.9	7,743.9	7,686.0	5,473.9
Temperature: inlet*, °C	26.50			26.27		
outlet, °C	26.72	26.75	26.75	26.41	26.43	26.45
RSD†, %	7.25	5.41	7.35	3.83	4.42	3.26

\*Input data

†Relative standard deviation from uniform flow distribution

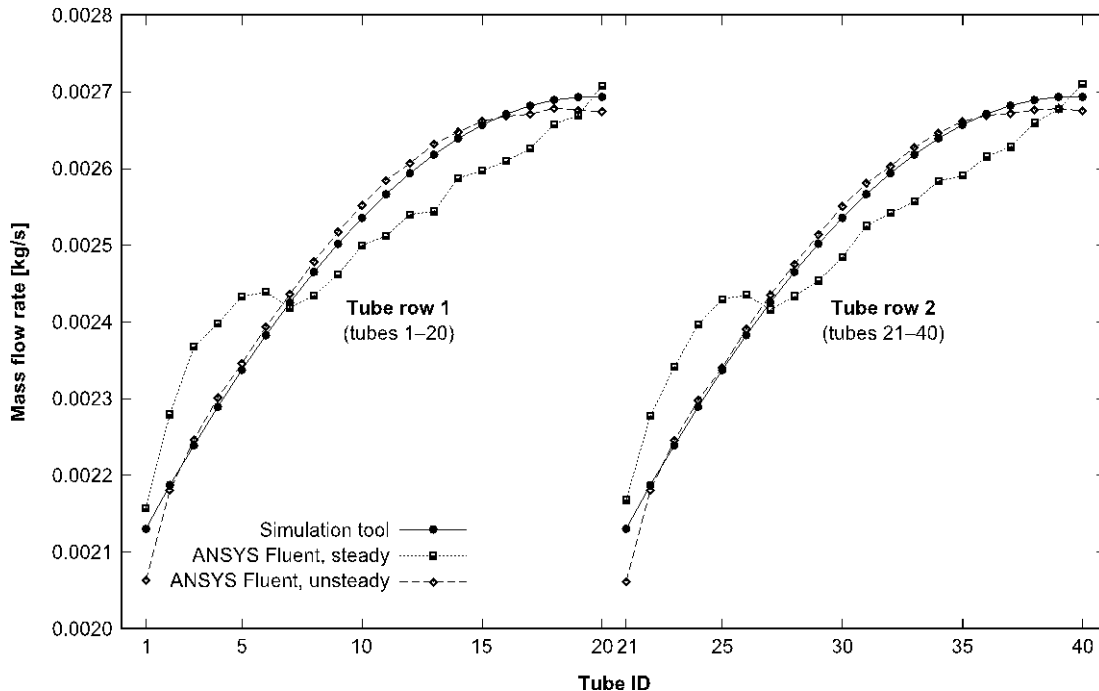


Figure 4: Tube mass flow rates for the first test flow system

Considering the first test system, from Figure 4 it is obvious that there is a strong agreement between the tube mass flow rates reported by the simulation tool and those yielded by the unsteady ANSYS Fluent model. The difference in reported pressure drops, however, is not negligible (1,919.8 Pa vs. 1,128.9 Pa

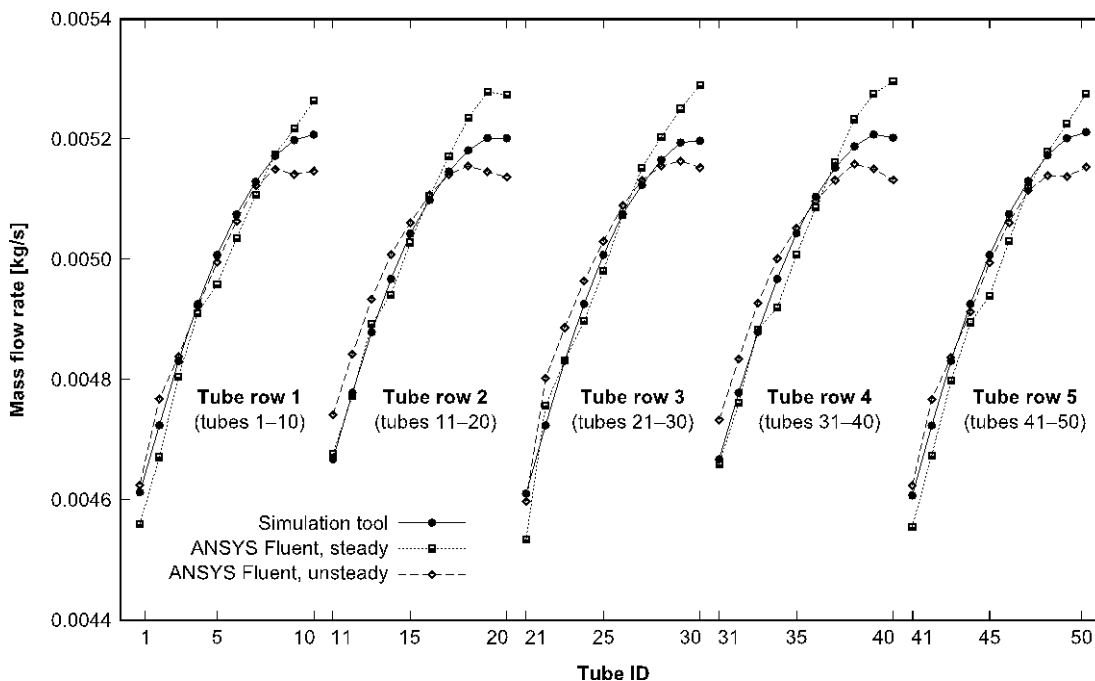


Figure 5: Tube mass flow rates for the second test flow system

in case of the simulation tool and ANSYS Fluent). In other words, although the flow distribution data match CFD results very well, the disparity between pressure drops warrants further investigation. As for outlet temperatures, all three models provided values which were higher than inlet temperatures even though there was no heated surface present in the system. This was simply due to energy dissipation. In any case, outlet temperatures were almost identical (26.72 °C according to the simulation tool vs. 26.75 °C according to ANSYS Fluent) with the actual temperature differences (inlet vs. outlet) varying by less than 15 %.

Results pertaining to the second test system (see Figure 5) show somewhat larger differences between what was obtained with the simulation tool and the data reported by the unsteady ANSYS Fluent model but the agreement still remains quite good. Here, however, the steady-state results seem far less erratic than they were for the first test system. In terms of pressure drop, the situation is similar as before – again the value reported by the simulation tool (7,743.9 Pa) is decidedly larger than what we obtained using the unsteady ANSYS Fluent model (5,473.9 Pa). Interestingly enough, pressure drop reported by the steady CFD model (7,686.0 Pa) is very close to what we got with the simulation tool now that – trend-wise – the mass flow rates reported by the steady CFD model are much more similar to those provided by the unsteady model. Considering temperature differences, the situation is akin to the previous case, that is, the provided outlet temperatures are almost identical (26.41 °C according to the simulation tool vs. 26.45 °C according to the unsteady CFD model).

In both the above mentioned test cases the times required to obtain the results with the developed Java application and ANSYS Fluent were vastly different. The application implementing the present model was able to provide results in times on the order of tens of seconds on a regular office computer (Intel Core i5-2500K CPU, single-thread computation). ANSYS Fluent, on the other hand, needed several hours to finish steady computation on a cluster while utilising eight or more CPU cores simultaneously. As for unsteady computations, they always ran for several additional tens of hours in order to reach fully converged states from the initial steady-state data. Memory requirements of both the simplified and CFD approaches were – obviously – greatly disparate as well due to the sizes of the employed meshes (hundreds to thousands of nodes in case of the simulation tool vs. millions of cells needed by ANSYS Fluent for  $y^+$  values being acceptable).

It should also be mentioned that many other test cases were evaluated (30 in total) with varying arrangements, header box dimensions, numbers of tube rows, numbers of tubes in each row, etc. Although we found that with increasing number of tube rows the differences between mass flow rates obtained with ANSYS Fluent and mass flow rates obtained with the simulation tool generally increased, the reported discrepancies remained quite small for any reasonably-sized tube bundle. It can therefore be said that in spite of its simplified nature the present model performs rather well.

Last but not least, we must emphasize the necessity for unsteady computations when models of systems in which one expects fair amount of turbulence are validated via CFD. With respect to the results illustrated in Figures 4 and 5 it is obvious that the utilised steady  $k$ - $\epsilon$  model was not capable of fully taking into account the turbulent nature of the flow (which, after all, is understandable given the amount of time-dependent information that simply cannot be included into a steady model). In other words, fitness of the steady-state computation approach which unfortunately still prevails in engineering practice should be reconsidered even at the cost of running computationally more expensive simulations.

#### 4. Future work

There are two main areas in which improvement is possible. First, one must consider the reported pressure drops being notably larger than those yielded by ANSYS Fluent. Second, though in terms of flow distribution the model performs rather well, the accuracy could still be higher in case of flow systems with larger numbers of tube rows.

We have also not yet tested how the present model performs if the tube bundle is sparse, i.e., if the longitudinal and transversal tube pitches are not reasonably small. In spite of the fact that the model explicitly assumes this not to be the case, it would be good to know whether this model can be safely used even in the requirement on tube bundle density is not satisfied.

So far the model has been validated solely via CFD and for distribution-only flow systems with air being the process fluid. While it is reasonable to expect the performance to remain more or less the same in case of other fluids and complete parallel flow systems, the respective validations should still be carried out. Moreover, it would certainly be beneficial to also utilise data from physical experiments for this purpose.

#### 5. Conclusions

It has been verified that – after the necessary modifications – the original quasi-1D partial differential flow model by Turek et al. (2014) can provide very good results even if applied to a quasi-3D mesh. Nonetheless, data obtained in the course of evaluation of test geometries via the developed simulation tool indicate that although flow distribution is predicted with good accuracy, there still is room for improvement in terms of pressure drop. What is more, additional validation steps are necessary to make sure the model can be safely used for geometries with sparse tube bundles as well as complete parallel flow systems.

#### Acknowledgement

The authors gratefully acknowledge financial support provided by Technology Agency of the Czech Republic within the research project No. TE02000236 “Waste-to-Energy (WtE) Competence Centre”.

#### References

- ANSYS Inc., 2013, ANSYS Fluent User’s Guide. ANSYS, Inc., Canonsburgh, USA.
- Galindo-García I.F., Vázquez-Barragán A.K., Rossano-Román M., 2014, CFD simulations of heat recovery steam generators including tube banks, ASME 2014 Power Conference, Baltimore, MD, USA, POWER2014-32261.
- Kim N.-H., Byun H.-W., 2013, Effect of inlet configuration on upward branching of two-phase refrigerant in a parallel flow heat exchanger, *Int. J. Refrig.* 36, 1062–1077.
- Mohammadi K., Malayeri M.R., 2013, Parametric study of gross flow maldistribution in a single-pass shell and tube heat exchanger in turbulent regime, *Int. J. Heat Fluid Fl.* 44, 14–27.
- Oracle, 2015, What is Java? <[www.java.com/en/download/whatis\\_java.jsp](http://www.java.com/en/download/whatis_java.jsp)>, accessed 20.02.2015.
- Osley W.G., Drögemüller P., Ellerby P., Gibbard I., 2014, Computational fluid dynamics investigation of air cooled heat exchangers, *Chem. Eng. Trans.* 39, 1351–1356.
- Pustynnik L., Barnea D., Taitel Y., 2010, Adiabatic flow distribution of gas and liquid in parallel pipes – effect of additional restrictions, *Chem. Eng. Sci.* 65, 2552–2557.
- Turek V., Bébar L., Jegla Z., 2014, Simplified pressure drop and flow distribution modeling in radial catalytic converters, *Chemical Engineering Transactions*, 39, 853–858.
- Turek V., Hájek J., Jegla Z., Stehlík P., 2011, Optimum design of fluid distribution systems in heat exchangers, *Asia-Pac. J. Chem. Eng.* 6, 750–759.
- Zhang Z., Mehendale S., Tian J., Li Y., 2015, Fluid flow distribution and heat transfer in plate-fin heat exchangers, *Heat Transfer Eng.* 36, 806–819.